

# Electrical Mechanisms (EMECS): Design Methods and Properties

G. N. Srinivasa Prasanna, International Institute of Information Technology,  
 26/C, Hosur Road, Opposite Infosys Technologies, Electronics City, Bangalore 560100  
 Corresponding Author: gnsprasanna@iiitb.ac.in

**Abstract:** In our earlier work [22], we have presented a synthesis of electrical machines and mechanisms, and presented a new set of devices called electrical mechanisms (*emecs*). In emecs irregularly shaped magnets are attached to different parts of the mechanism, and provide customizable tangential forces in different configurations. The presence of these tangential forces differentiates emecs from other mechanisms. In this paper we present a simple method to design these magnets based on integral equations. We show that properly designed emecs offer surprising properties - we can design slider-crank mechanisms which can present oscillatory forces to the load, even when driven by a constant force.

**Keywords:** Margins, Tables, Figures, and Equations

## 1. Introduction

Our earlier paper [22] generalized the concept of motors to electrical mechanisms (emecs). As opposed to motors, which are revolutes or prismatic pairs enhanced with magnets (permanent, electromagnets), emecs are entire mechanisms enhanced, in various places with magnets. In general the magnets are irregular in shape and size, and the device cannot be regarded as a set of linear/rotary motors driving a mechanism. The magnetically enhanced joints (pairs) in emecs are called *epairs*.

This paper presents a simple *design method* to design primarily the passive components of emecs in a systematic fashion. Methods of active control will be dealt with in future papers. Our methods rely on integral equation formulations (or their discretized linear equation equivalents). **We show that properly designed emecs show surprising properties – a slider crank can show oscillatory output torque, even with a constant force at the slider. We can design a magnetic flywheel for an IC engine, which can ideally reduce torque ripple to zero (it was non-zero in our heuristically designed IC engine flywheel in [22]).**

We believe our work is the first to do a systematic synthesis of electrical prime movers and mechanisms, and present systematic design methods for the same. Comparison with the state-of-art is in Appendix-A (we are unaware of any directly related work). The work is applicable generally, in robots, automobiles, aircraft, spacecraft, etc. The power levels are comparable to medium power pneumatics (see the discussion in [22]).

This paper summarizes the architecture of emecs (elaborating our previous discussion in [22]), introduces im-

portant design principles, and finally presents a detailed example of the capabilities of a properly designed slider-crank emec. First, we illustrate the concept through the simplest of emecs, a prismatic pair, showing an integral equation formulation for the design (Section 2). The structure and design of emecs follows (Section 3). A detailed discussion of the slider-crank follows (Section 4), and then conclusions (Section 5).

## 2. A simple EMEC

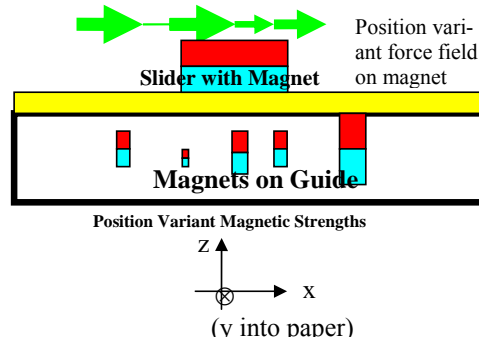


**Figure 1 Synthesis of arbitrary position variant tangential force using position variant magnetic strengths, interacting with a fixed magnet.**

We use a simple example to illustrate the idea of an emec. Figure 1 shows a simple emec, composed of a single prismatic pair, enhanced with magnets on both the guide and the slider. We wish to control the motion of the slider, of mass  $m$ , w.r.t the guide. Newton's law is

$$m\ddot{x} = F_{tot}$$

where  $F_{tot}$  is the total force acting on the slider, from all sources. If the total applied force is constant, so is the acceleration of the slider.

In many circumstances, however, it is desirable to have a constant force resulting in a non-constant acceleration, or a non-constant force resulting in a constant acceleration. For example, in a vibration jig, the acceleration of the table holding the object should have all frequency components upto the maximum vibration frequency to be tested. It is preferable that the prime mover driving the jig should work at a constant force/torque output.

How is this possible? For a non-constant acceleration, the total force has to be non-constant (assuming the mass is constant, which is true in mechanisms we discuss here). However, if a portion of this force is provided by the internal structure of the mechanism, then

the acceleration of the slider can be non-constant, even if the *applied external force* is constant. An emec achieves this by using *internal electromagnetic forces*, which are non-contact, repeatable, and are approaching power levels of medium power pneumatics. **The internal electromagnetic force is tangential to the contact surfaces, differentiating emecs from all other mechanisms, and leads to some surprising properties.** There are also normal forces due to the magnetics, but for the class of emecs considered, these can be subsumed in the contact reactions, and do not figure in the dynamics. Emecs having global interactions require these forces to be accounted for, but this is outside the scope of this paper.

Considering the prismatic pair again, let us denote the internal force by  $F_m$ . Then Newton's law becomes (for time and position dependent forces):

$$m\ddot{x} = F_{tot}(x, t) = F_{ext}(x, t) + F_m(x, t)$$

An appropriate *tangential*  $F_m(x, t)$  can enable a desired acceleration for a given external force. In the emecs we consider, this force is generated by the differently sized magnets interacting with each other<sup>1</sup>, is time invariant, but changing as a function of position (see Figure 1). This change of tangential internal force w.r.t position is critical to the emec, and accounts for its properties.

### Prismatic EMEC versus Linear Motor

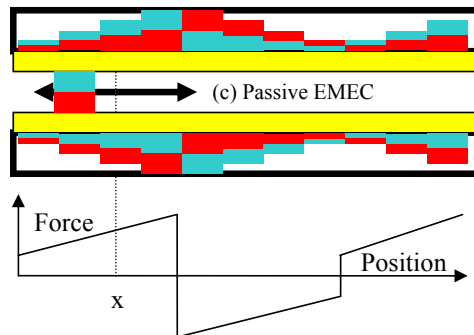
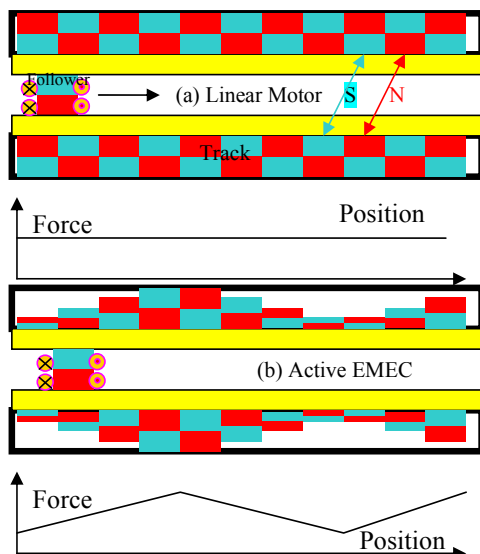


**Figure 2 (a) Linear Motor versus (b) Active Prismatic EMEC. Coils are present only on the follower (moving member). (c) Passive EMEC**

It is illustrative to compare a linear motor with a prismatic emec in more detail. Figure 5 compares a linear motor with its closest comparable emec – the prismatic epair. Figure 2(a) shows a simplified linear motor. Regularly spaced permanent magnets in the track interact with the electromagnet in the follower. By a proper phasing of the current in the follower (polarity reversal after each pole piece is crossed), a constant (roughly) forward force is generated on the follower. The residual ripple in the force can be smoothed out by another follower which is offset by half a pole pitch, and mechanically connected to the one depicted, as is well known in the design of linear motors (reduction of cogging torque).

Figure 2 (b) shows a prismatic active emec. Unlike the linear motor, the pole pieces are not of the same magnetic strength. The strength increases and decreases in a “sinusoidal” fashion with position (in general the spacing can be irregular too). With the same excitation as before, the forward force increases and decreases in a sinusoidal fashion.

Finally, Figure 2(c) shows a completely passive prismatic emec. At any position, say “x”, the net force is the difference between the backward pull of the (smaller) magnets to the left of x, and the forward pull of the (larger) magnets to the right, and is *related to the slope of the magnetic strength curve*. A positive slope implies a forward force, and a negative slope a backwards force. The total forward force summed over all positions is zero, since the system cannot provide net energy.

Why do we need such *position variant* structures? In short, *to compensate for nonlinear mechanism and prime mover dynamics* which change as a function of position/ configuration. At those positions where the prime mover forward force (as reflected through the mechanism position function) is weak, the passive emec can add to the forward force, and vice versa in those positions where the prime mover is excessively strong.

<sup>1</sup> There are other means of generating these forces, e.g. attraction between magnets and magnetic materials, eddy/hysteresis effects, etc, but this is out of scope of this paper.

An IC engine furnishes an excellent example. At top dead center (TDC), the combustion is just starting, and the crank is in line with the connecting rod resulting in a small lever arm. Due to both effects, the net torque delivered is zero. Further into the cycle, the combustion completes, and the lever arm is also large, resulting in a torque much larger than the mean torque. Further into the cycle, during compression (just before TDC), the net torque delivered is negative, and energy is absorbed by the engine from the flywheel. This position variant torque can be smoothed by putting a magnetic position varying load, which absorbs/releases energy losslessly with the IC engine (Section 4).

### Synthesis of Fields and Forces

The fundamental way a position variant magnetic force is generated is by generating a position variant magnetic field. The field produced by a single elementary magnet shows a fixed variation with distance – approximately inverse square. *Arbitrary* position variant magnetic fields (not inverse square) in general require multiple magnets whose size, material strengths, etc varies with position, i.e., a *spatial* distribution of magnets (Figure 3). The spatial distribution of magnets can be calculated as follows.

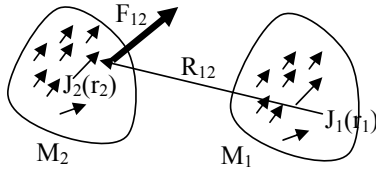


**Figure 3 Force between two magnets represented by current distributions**

First, the origin of magnetic fields can be identified as current densities  $\overline{J}(\overline{r})$  (or magnetic moments, this is equivalent) in space. Two interacting magnets  $M_1$  and  $M_2$  can hence be identified by associated current densities  $\overline{J}_1(\overline{r}_1) = \overline{J}_1(x_1, y_1, z_1)$   $\overline{J}_2(\overline{r}_2) = \overline{J}_2(x_2, y_2, z_2)$  in their respective regions. These current densities depend on the materials used for these magnets. Using the Biot-Savart law [23][24], the magnetic field  $B$  and forces  $F_{12}$  acting on  $M_2$  due to  $M_1$  as arranged in Figure 3 are given by the relevant cross products:

$$B(\overline{r}_2) = \frac{\mu_0}{4\pi} \int \overline{J}_1(\overline{r}_1) \times \frac{\hat{r}_{12}}{R_{12}^2} dV_1, \text{ Teslas}$$

$$R_{12} = |\overline{r}_2 - \overline{r}_1|, \hat{r}_{12} = \frac{|\overline{r}_2 - \overline{r}_1|}{R_{12}} \quad (1.1)$$

$$F_{12} = \int \overline{J}_2(\overline{r}_2) \times B(\overline{r}_2) dV_2 \text{ Newtons}$$

From Equation (1.1), the *elemental* force between an elemental current density comprising the magnet  $M_1$ ,  $\overline{J}_1(\overline{r}_1)$  at location  $\overline{r}_1$ , and the elemental current density

comprising the magnet  $M_2$ ,  $\overline{J}_2(\overline{r}_2)$ , at location  $\overline{r}_2$ , depends on the vector displacement between them  $R_{12} = |\overline{r}_2 - \overline{r}_1|$ . Since we are discussing a 1-D prismatic pair, this reduces to the distance between the elemental currents,  $x_{12} = x_2 - x_1$ . The total force  $F_{12}$  between the magnets  $M_1$  and  $M_2$  is the integral of all these elemental forces, over both the regions enclosed by the magnets.

Now, in our prismatic pair,  $M_1$  is rigidly attached to one link, and  $M_2$  to the other. As the links slide against each other, the force  $F_{12}$  changes, due to the change in the elemental forces. The change in the elemental force is due to the change in the distance between two elemental current densities

$$x_{12} = x_2 - x_1 \rightarrow x'_{12} = x'_2 - x'_1$$

where the primes denote the new positions. We assume that the currents are constant – we are discussing permanent magnets here. Since the motion is rigid, the change in distance is the *same for all pairs of elemental current densities*, and can be equated to the change in distance  $x$  between a reference point on the first magnet  $M_1$  and a reference point on the second magnet  $M_2$  (say centroids).

$$x'_{12} = x'_2 - x'_1 = x_{12} + x$$

We use “ $x$ ” instead of “ $\Delta x$ ”, for reasons which will be clearer below. Given an  $x$ , the relative position of the magnets is completely specified. Then, from Equation (1.1) when the links slide, the field  $B$  is a function of *both*  $x_2$  and  $x$  ( $x_1$  is integrated out), but force  $F_{12}$  is *only a function of  $x$*  ( $x_1$  and  $x_2$  are integrated out), and the current densities (or equivalently magnetic moments) in the magnets. We can write:

$$B(x_2) = B(x_2, x)$$

$$F_{12}(x_1, x_2) = F_{12}(x = x_1 - x_2) = \kappa \left( \int J_1, \int J_2 \right) f_{12}(x) \quad (1.2)$$

Where  $\kappa \left( \int J_1, \int J_2 \right)$  depends on the *integrals of the elemental current densities* or equivalently magnetic moments in the magnets. Equation (1.2) is intuitive – the force between two magnets depends only on (a) the magnetic moments inside the magnets and (b) the separation between them, in a 1-D setting (in a 3-D setting, the relative orientation also matters). If the force  $F_{12}$  is specified at all relative distances, the resulting integral equation can be solved to yield the current densities  $J_1, J_2$ , at all points in the interior of both magnets. This is the basis of our approach.

However, a simpler form of Equation (1.2) suffices for our 1-D prismatic pair. From the third equation of Equation (1.1), and the first equation of Equation (1.2), it is easy to see that (see Figure 4):

$$F_{12}(x_1, x_2) = F_{12}(x = x_1 - x_2) =$$

$$\int J(x_2) B(x_2, x) dx_2 = \quad (1.3)$$

$$\int J(x_2) B(x - x_2) dx_2$$

Here we have used the fact that  $\overline{B}(x_2)$ , the field density per unit length, produced at location  $x_2$ , depends only on the distance from the reference point on  $M_1$  to the current location  $x_2$ , which is  $x-x_2$ .

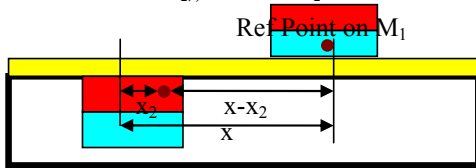


Figure 4: Geometry of force production

The intuition is that the force on magnet  $M_2$  due to  $M_1$  at a distance  $x$ , is composed of the sum of all the elemental forces produced by a (linear) current density at  $x_2$ , multiplied by the field strength at that point, which is at a distance  $x-x_2$  from reference point on magnet  $M_1$  (Figure 4). This is a convolution integral. With a slight change of notation, this can be re-written as the sum of elemental forces produced per unit length on a unit current  $J_2$  at  $x_2$ ,  $f(x-x_2)$  multiplied by the ratio of the actual current density to a unit current:

$$F_{12}(x) = \int K_2(x_2) f(x-x_2) dx_2 \quad (1.4)$$

We shall denote  $f(x)$  as the *kernel* (Newtons per meter), and the dimensionless ratio  $K_2(x_2)$  will be called the *equivalent strength*. In many cases, we have a finite number of magnets (not a continuous distribution) and Equation (1.4) changes to.

$$F_{12}(x) = \sum_i K_i f(x-x_i) \quad (1.5)$$

Here the kernel is a force (Newtons) and can be computed by finite-element methods, given the shape and properties of  $M_1$ . We shall discuss how to determine the equivalent strengths below.

We note that the convolution integral is valid in this form only for a 1-D pair. For 2-D and 3-D structures, magnet orientation enters the equations too, and Equation (1.2) does not reduce to such simple forms.

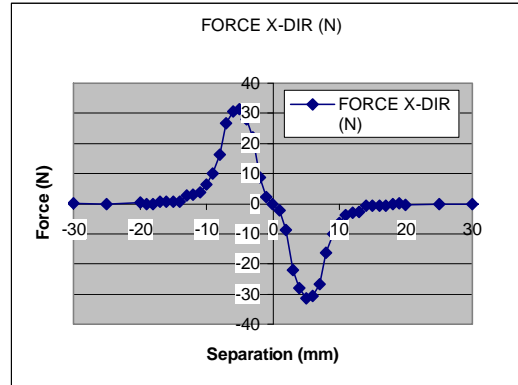
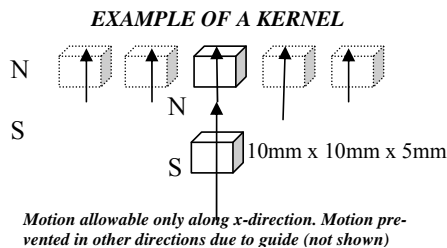


Figure 5 Example of a kernel showing horizontal component of force.

An example kernel determined by finite-element analysis (FEM) is shown in Figure 5, where two 10 mm x 10 mm x 5 mm magnets are shown, one attached to each link in the prismatic epair. Opposite poles face each other, resulting in attractive forces between the magnets. The vertical separation is 1 mm (air gap). The horizontal separation varies. When the top magnet is far to the left (more than 20 mm apart), the interaction is weak, and the horizontal force in the positive x direction is weak. As it approaches, the horizontal force first increases, peaks at 30 N at 5 mm separation, and then rapidly goes to zero when the magnets are right on top of each other (here the force is vertical). The force reverses direction after the top magnet slides past the bottom one. The integral of the force is zero, because the system is passive.. In general, Modern Neodymium magnets are powerful enough to offer 10's of Newton's of force at a few mm separation, with structures only a couple of cm<sup>2</sup> in area.

### 3. Optimization of Equivalent Strengths

Generating/computing an appropriate kernel is only half the story. The other half is to determine and synthesize magnetic structures with the correct equivalent strengths as per Equation (1.4) or(1.5). Determining optimal equivalent strengths is discussed in detail below. But first we mention a couple of points regarding realization of equivalent strengths of the magnets involved:

- One method is to use different materials, and keep the same dimensions. It is easily seen from first principles, that if the B-H curve is scaled by a factor of  $N$ , all fields scale up by a factor of  $N$ , and forces by a factor of  $N^2$ . The same effect can be obtained by changing the air gaps in the flux paths.
- Alternatively, the dimensions of the magnets can be chosen to generate specified equivalent strengths (using FEM analysis).

Even after generating an appropriate kernel, and with the ability to accurately synthesize equivalent strengths, every force profile cannot be exactly synthesized. There

is *residual error*, which can be minimized by choosing optimal equivalent strengths.

We show below that an optimal profile of equivalent strengths can be selected using methods of convex optimization [25]. The error in force at each position-, can be expressed as a convex function of the equivalent strengths. Various criteria can be used – minimization of the mean-square error over all positions ( $L_2$ ), minimization of the maximum error over all positions ( $L_\infty$ ), etc.

Our notation is as follows.  $f_{\text{target}}(x)$  is the force as a function of  $x$ , targeted to be synthesised,  $f_{\text{synth}}(x)$  is the synthesized force, and the kernel is denoted by  $f(x)$ , and is obtained apriori from FEM analysis. The error at each position  $x$  is  $\text{Err}(x)$ . The optimization can include limits on equivalent strengths, due, say to manufacturing constraints. Other constraints (sums, differences, etc) on equivalent strengths can also be included if required.

The optimization procedure is given below:

$$\min_K E_2 \text{ or } E_\infty$$

Subject to:

$$E_2 = \int \text{Err}^2(x) dx, E_\infty = \text{Max}_x (\text{Err}(x))$$

$$\text{Err}(x) = \left| f_{\text{synth}}(x) - f_{\text{target}}(x) \right| \quad (1.6)$$

$$f_{\text{synth}}(x) = \int K(x') f(x-x') dx'$$

Under Constraints:

$$\text{Bounds : } K^{\min} \leq K(x) \leq K^{\max}$$

Other Constraints on  $K$ 's

Equation (1.6) is written for a continuous profile of magnets. For a discrete set of  $N$  magnets, the integrals are replaced by sums. Since the objective function ( $L_2$  or  $L_\infty$ ) is convex w.r.t  $K$ , and the constraints are also convex (bounds, and other convex constraints) Equation (1.6) specifies a convex optimization, solvable using state-of-art solvers like CPLEX. In our discussion below, we discretize the synthesized force at  $M$  equally spaced positions  $x_i$ . The synthesized force at different positions  $x_i$  can be then written as a matrix equation

Specification at  $M$  points, with  $N$  Magnets:

$$i=1..M, j=1..M$$

$$\overline{f_{\text{synth}}(\vec{x})} = [F_{ij}]_{M \times N} \vec{K}$$

$$\vec{x} = [x_1, x_2, \dots, x_m]^T$$

$$F_{ij} = f(x_i - x_j) \Delta x, \Delta x = \frac{x_{\max} - x_{\min}}{N}$$

$$\vec{K} = [K_1, K_2, \dots, K_N]^T$$

$$\overline{f_{\text{synth}}(x)} = \left[ f_{\text{synth}}(x_1), f_{\text{synth}}(x_2), \dots, f_{\text{synth}}(x_m) \right]^T$$

(1.7)

In the absence of constraints on  $K$ , singular-value-decomposition (SVD) can be used in Equation (1.7), for minimizing the squared error. The max error can be minimized using Linear Programming. In the general case, where constraints are present a convex optimization solver is required. The output of this optimization is a specification of the equivalent strengths of all magnets in this prismatic pair.

While Equation 1.6 is written with respect to a prismatic pair, it is evident that the same equations (with changes from linear position  $x$  to angular position  $\theta$ , torque instead of force, if required) can be used for any of the epairs in an emec. We shall use it for a revolute pair in Section 5:

What force profiles can be generated thus? From Equation (1.4), taking (spatial) Fourier Transforms

$$F_{\text{synth}}(jw) = K(jw) F_{\text{eq}}(jw) \quad (1.8)$$

The Fourier Transform of the synthesized force  $F_{\text{synth}}(jw)$  is the product of the Fourier Transforms of the kernel and the equivalent strength. Clearly the set of all derivable force profiles is spectrally limited to the spatial frequencies present in the kernel, and those in a realizable equivalent strength profile (maximum rate of change of magnetization direction and strength). Both are limited by manufacturing processes – the kernel's spatial frequencies are limited to the smallest magnetic domain which can be easily manufactured, and the equivalent strength by the sharpest change in magnetization orientation possible. Disk drive technologies are proof that spatial frequencies in *microns per cycle* can be constructed. The spectral approach can also be used for optimization in the spectral domain (details omitted).

## Epairs to Emecs

We have discussed the structure and design of the simplest emec, composed of a single epair. Based on Equation 1.6 we briefly discuss extensions to emecs composed of multiple pairs.

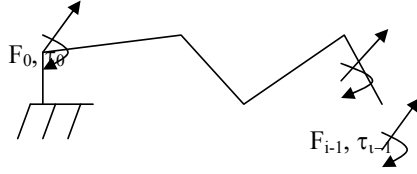


**Figure 6: Design of a Serial emec**

In Figure 6, we have a serial manipulator, in a certain configuration specified by inter-link angles ( $\phi_0, \phi_1, \phi_2, \dots$ ). For simplicity, we treat a planar emec, but the results generalize for a general 3-D emec, with more configuration parameters. The force/torque at joint I is given by  $F_i$  and  $\tau_i$  respectively, and can be determined as a function of the end-effector forces/torques at this configuration, using standard kinematic equations [1][2][3][4]. As per Section 2, the normal forces due to the magnetics in epairs can be ignored, and the design of the emec reduces to designing each epair with specified tangential forces/torques each configuration, as per Equation(1.6). The design of parallel manipulators is similar, with the additional constraint that the forces/torques have to be partitioned amongst the different paths leading to the end-effector.

## 4. Applications

We present an analysis of the dynamics of the important slider-crank emec (i.e. a slider-crank mechanism enhanced with magnets at various places). **Our major conclusions are that the output force need not be related to the input force through the mechanism's transfer function, but can be within limits arbitrary.** This offers new features in the design of mechanisms, wherein dynamics can be partly decoupled from kinematics.

The output force/torque of an emec is the combination of the input force/torque, reflected through the mechanism position function, together with internal magnetic forces/torques. The output force/torque in general changes with mechanism configuration. This changing force/torque will be called the output force/torque function of the emec. We show that emecs can have a wide range of output force/torque functions, limited primarily by the *spatial resolution* of the magnetic kernel. Unlike classical mechanisms, the input torque/force and output force/torque are **not related by a geometric/kinematic parameter** (e.g. in a lever/gear etc), but depend on the magnetic field strength, which is independent of kinematics (as long as the magnetics fits inside the space provided by the mechanism in all its positions). The dynamics can even be changed, by changing the magnetics, while keeping the rest of the mechanism invariant.

We discuss a lossless slider-crank emec, so that the input power is completely and instantaneously transferred to the output, *if the magnetic energy storage was absent*. We also assume that the mechanism is moving slowly, so that electromagnetic wave effects are negligible (quasi-static - true in most cases). The *temporal* (not spa-

tial) bandwidth of our slider-crank emec is hence infinite. Spatial bandwidth is discussed in detail below.

## Slider-Crank Mechanism

We shall discuss the behaviour of the slider-crank emec in Figure 7 when a force is applied to the slider and output torque taken from the crank (e.g. an IC engine). The opposite case, where the crank is driven is omitted for lack of space, but is qualitatively similar. The structure of the mechanism imposes a zero output function at the mechanism positions corresponding to top and bottom dead centers (TDC/BDC).

A slider-crank (Figure 7) can be converted into an emec by adding magnets at one or more of the following:

- The revolute pairs (crankshaft bearing A and the crank pin B in Figure 7)
- The prismatic pair (slider C) and its pin D to the connecting rod.

In case (b) the reciprocating motion of the prismatic pair and its pin imposes a half-period symmetry. The magnetic forces/torques generated in the second half cycle are time reversed copies of those generated in the first half cycle. No such constraint is present for the revolute pair on the crank axle (and its pin). Hence, for maximum flexibility, we discuss enhancement of the crankshaft (it can be shown that enhancement of the crank pin does not lead to new capabilities).

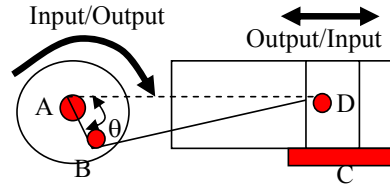


**Figure 7: Slider-Crank Mechanism with Enhanced Magnetics on both crank axle and slider (red)**

We discuss the customizability of our slider-crank emec, based on a *spatial* Fourier Decomposition of the output force, given a constant force in the direction of motion. If a sinusoidal output of a given spatial frequency can be synthesized, any output function having spatial frequencies upto this bandwidth can be synthesized using superposition of magnetic structures corresponding to each spatial frequency. This is based on the linearity of Maxwell's equations, and approximate linearity of magnetic materials (details are skipped for brevity).

To keep the discussion simple, we shall assume that the connecting rod is long, so the force  $F$  on the slider and the torque  $\tau$  on the crank are related by

$$\tau = F \sin(\theta)$$

where  $\theta$  is the angle of the crank from the line joining the centers. The discussion does not change qualitatively for short connecting rods. The torque on the load is given by

$$\tau = F \sin(\theta) + \tau_m$$

where  $\tau_m$  is the magnetic correction to the raw torque  $F \sin(\theta)$ . A specified force  $F_{spec}(\theta)$  should result in a specified synthesized torque  $T_{spec}(\theta)$ , using magnetic kernels  $\tau(\theta)$ . The magnets are designed using the discrete version of Equation (1.6) for torque synthesis, with  $N$  magnets equally spaced in angle, and error evaluated at  $M$  points  $\theta_k$ :

$$k = 1 \dots M; M \geq N$$

$$T(\theta_k) \approx \sum_{j=0}^{N-1} K(\theta_j) \tau(\theta_k - \theta_j) \Delta\theta; \Delta\theta = \frac{2\pi}{N}$$

$$\tau_{err}(\theta_k) = \tau_m(\theta_k) - (T_{spec}(\theta_k) - F_{spec} \sin(\theta_k))$$

Our approach will be to design magnetics for  $T_{spec}(\theta_k)$  of various spatial frequencies and amplitudes. Optimization to minimize the error (either mean-square –  $L_2$  – or max -  $L_\infty$ ) is done using SVD techniques, as per Section 3, since we do not have constraints on equivalent strengths for our examples.

Our kernel is a scaled version of Figure 4, and dimensioned [22] such that it is effective for use in torque smoothing of an IC engine working at 1KW at 2000 RPM – it occupies an angular extent of 2 degrees at 10 cm radius. The spatial spectrum (not shown) has significant frequencies till 30 cycles/revolution. Hence we expect our designs to be able to match any torque function having components till 30 cycles/revolution, and this is indeed the case (these results are not shown for brevity).

Here, since we deal with fundamental capabilities of emecs, we present only normalized results, and results with actual dimensions indicate power-size levels approaching medium-power pneumatics for comparable dimensions (see the photograph in Figure 12).

We illustrate how magnetics can smooth the jerky torque produced by a slider-crank driven by a constant force (in direction of motion). The crank torque corresponding to a constant force input at the slider is shown in Figure 8, and is a rectified sine wave. By proper magnetics, this rectified sine wave can be converted to sine wave of any desired *different frequency and desired amplitude* (within limits), as long as the average torque per cycle is kept invariant (for a passive emec).

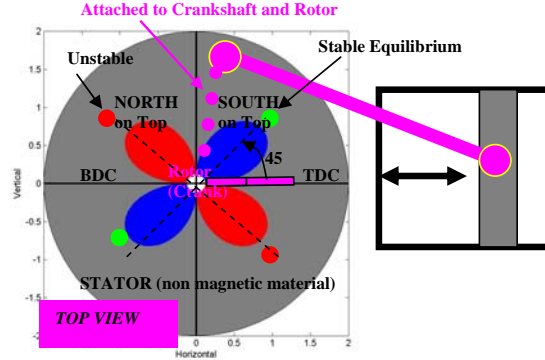
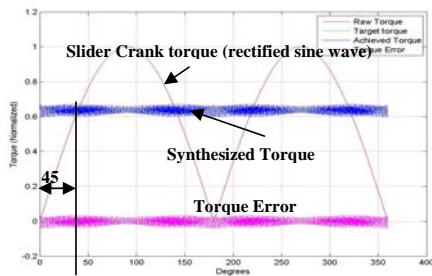


**Figure 8 (a) Torque function and (b) Magnetic Structure for zero target ripple (TOP VIEW). Connecting Rod is attached to Rotor structure**

Figure 8 (a) shows the raw torque (rectified sine-wave purple), the synthesized torque (blue) and the error (magenta) for zero target ripple (constant torque). Figure 8 (b) shows the magnetic structure. When used in an IC-engine, the **Rotor is attached to the crankshaft, and stator is attached to the engine block** (stationary). The stator is composed of a disk of non-magnetic material, into which magnets of varying sizes are inserted in the “butterfly-shaped” areas. Red colour indicates North on top of the stator, and Blue South on top of the stator. The Rotor is on top of the stator, is composed of a long magnet, with North *facing the stator*. Hence the rotor is attracted to the blue areas (having South on top), and repelled from the red areas (having North on top). The rotor magnet is attracted more where the stator has a larger magnet (more blue)<sup>2</sup>. The total force is given by the signed sum of the torques due to the interactions between the rotor and stator magnets, and is related to the slope of the stator magnetic profile curve, as per Section 2. The magnetic profile of the stator has been designed to exactly cancel the torque ripple of the slider-crank, as further explained below. The residual ripple of a few percent is due to the finite number of magnets (180). It will vanish if we use a continuously variable magnetic profile.

In Figure 8 (a) till 45 degrees, the mean torque is greater than the torque delivered by the slider-crank, and requires the magnetics to *add* to the output torque. The amount of additional torque is large at 0 degrees, but decreases to zero at 45 degrees. In Figure 8 (b) the rotor, having NORTH at the bottom faces the south poles on the stator between 0 and 45 degrees. The *size* of the stator magnets increases with angle, but with a gradually decreasing slope. The exact slope and the size of the magnetized area on the stator depends on the shape and magnitude of the kernel. As per the discussion in Section 2, a forward force, decreasing with angle results, as required. The operation of this butterfly magnetic structure during the rest of the cycle can be understood on

<sup>2</sup> There are other ways of doing this – more powerful materials, etc, as explained before – Section 3.

similar lines – comparing the required torque correction in Figure 8 (a), with the *slope and polarity* of the magnetic structure in Figure 8 (b).

The operation of this device can be understood by *energy exchange* between the magnetic field and the prime-mover. When the prime mover generates too much torque, the excess is stored in the magnetic field. When the prime mover torque needs augmentation, this pre-stored energy is released. This exchange repeats itself every cycle.

Stable equilibria, where the rotor comes to rest in the absence of prime mover force are marked in green, and unstable ones in red. The equilibrium at 45 degrees is stable, since just before this position, the force is counterclockwise, and clockwise just after this position.

Equally interesting is the 200% ripple case, where the ripple is *doubled* by the magnetics (say for a rotary vibrator). The magnetic structure is shown in Figure 9, and is almost 3 times as large as the zero ripple case. The magnetic profile is similar to the zero ripple case, but slightly offset in angle. This can be understood by looking at the required torque corrections in Figure 9(a).

Figure 10 (a) and (b) show a structure for converting the same slider crank, to a device having 150% torque ripple, and a *fractional* frequency of 2.7 cycles/revolution. The torque is ideally *discontinuous* at TDC, and this is shown by the sharp change in slope at TDC (in reality there is a non-zero transition region). Stable equilibria are marked in green, and unstable ones in red.

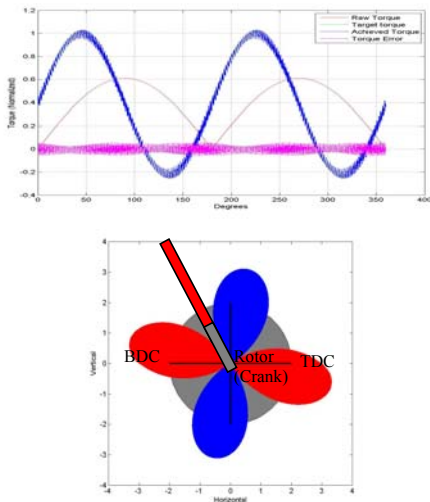


**Figure 9 (a) Torque function and (b) Magnetic Structures for vibration enhancing emec (doubles torque ripple).**

**Dynamics of these systems is complex.** In the simplest case of the system producing a constant output torque, the angular acceleration is constant, and the load moves

at a linearly increasing angular velocity. In the presence of torque ripple, at each angular position, the load sees different torques, leading to nonlinear dynamics. If the torque ripple has a single frequency, the resulting dynamic equation resemble the large amplitude oscillations of a pendulum, and can be integrated using Elliptic Integrals. Details are skipped for lack of space.

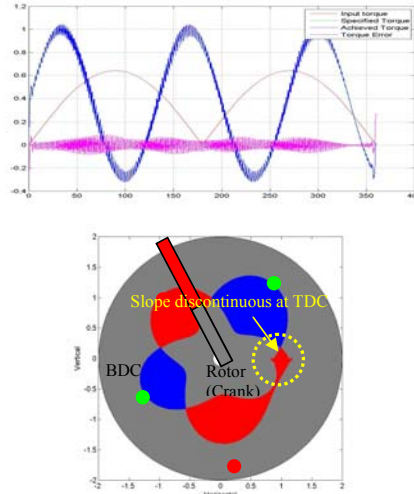


**Figure 10 (a) Torque function and (b) Magnetics for converting a slider-crank output to a sinusoidal variation of 2.7 cycles/revolution.**

### Torque Smoothing of 1 KW, 2-cylinder, 2-stroke engine.

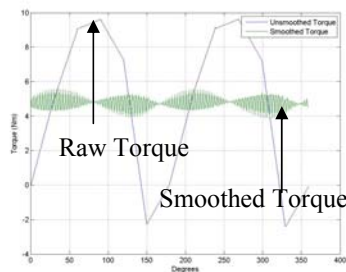


**Figure 11: Torque Smoothing for 1KW, 2-cylinder engine.**

Our ideas are practical. By properly putting magnets (structure is similar to those shown before) on an IC engine flywheel, we can reduce the torque ripple to zero. In Figure 11 the raw torque of a 2-cylinder 2-stroke engine ranges from 10 Nm during peak combustion, to -2 Nm during compression. By comparison, the smoothed torque with 180 magnets on the circumference of the flywheel produced by the SVD analysis shows an almost constant mean of 5Nm, ripple of 1.8Nm, together with a high frequency harmonic – this is caused by the finite

number of sectors used, and the resulting discrete changes in the magnetic strength.

This is being manufactured – the test jig shown in Figure 12 can hold an arbitrary flywheel (roughly 20 cm x 5 cm, unoptimized dimensions), and is instrumented with a Messerschmit 100 Nm torque sensor, to measure torque of an actual flywheel structure. Initial experimental results are promising, and full results will be available by the time of the conference.

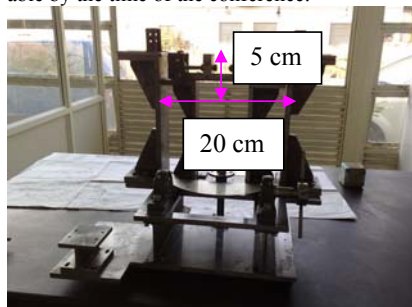


**Figure 12: Test Jig showing magnetic flywheel (dimensions unoptimized)**

Such structures have the following advantages over a normal flywheel

- The magnetic force angular profile can be designed to exactly cancel the residual torque ripple, and make the engine look like a constant torque prime mover
- The smoothing is speed invariant, and works at low speeds too, where a flywheel is ineffective.
- The magnetics is lighter and has less inertia than a flywheel.

## 5. Conclusions

We have analysed the output function (torque/force) of an emec. *The output function of emecs is not solely dependent on geometric parameters, but can be shaped by choosing appropriate magnetics.* Integral equation formulations applied to a slider-crank mechanism enable oscillatory output torques to be produced, with constant force input at the slider. Torque ripple of an IC-engine can also be ideally reduced to zero at all speeds. While details of *system dynamics* are in other papers, we note that our techniques can be used together with all currently known methods of mechanism dynamic control.

## References

- [1]. Ghoshal, A, *Robotics: Fundamental Concepts and Analysis*, Oxford Univ Press, 2006.
- [2]. Uiker, Pennock, Shigley, *Theory of Machines and Mechanisms*, Oxford, III Edition.
- [3]. A. Ghosh and A. K. Malik, *Mechanisms and Machines*, III Edition.
- [4]. Myszka, *Machines and Mechanisms: Applied Kinematic Analysis*, Prentice Hall, 2004.
- [5]. Nakamura, A. *Advanced Robotics, Redundancy and Optimization*, Addison Wesley, 1991.

- [6]. Kim, S, “Optimal Redundant Actuation of Close-Chain Mechanisms for High Operational Stiffness”, IEEE/RSJ Proc 2000 IEEE/RSJ Internl. Conf. on Intelligent Robots and Systems.
- [7]. Hirose and Arikawa, “Coupled and Decoupled Actuation of Robotic Mechanisms”, *Proc. of 2000 IEEE Intl. Conf. on Robotics and Automation*, San Francisco, CA, 2000.
- [8]. Press et al, *Numerical Recipes, the art of Scientific Computation*, Cambridge Univ Press
- [9]. Liang Yan; I-Ming Chen; Chee Kian Lim; Guilin Yang; Wei Lin; Kok-Meng Lee, “Design and Analysis of a Permanent Magnet Spherical Actuator”, *IEEE/ASME Trans on Mechatronics*, April 2008, pp 239-248.
- [10]. H.J. Van de Straete; J. De Schutter, “Hybrid cam mechanisms”, *IEEE/ASME trans. Mechatronics*. Dec 1996, pp 284-289.
- [11]. Ohnishi; M. Shibata; T. Murakami, “Motion control for advanced mechatronics”, *IEEE Trans Mech*, March 1996, pp56-67;
- [12]. S. Arimoto, T. Nakayama, “Another language for describing motions of mechatronics systems: a nonlinear position-dependent circuit theory”, *IEEE Trans Mech*, June ‘96, pp 168-180.
- [13]. Yamaguchi, T.; Numasato, H.; Hirai, H, “A mode-switching control for motion control and its application to disk drives: design of optimal mode-switching conditions”, *IEEE Trans Mech*, Sept 1998, pp 202-209.
- [14]. Dixon, W.E., “Adaptive Regulation of Amplitude Limited Robot Manipulators With Uncertain Kinematics and Dynamics”, *IEEE Trans. On Automatic Control*, March 2007.
- [15]. Boldea, I. Nasar, S.A, “Linear electric actuators and generators”, *IEEE Trans Energy Conversion*, Sept ‘99, Vol 14, Issue 3, pp 712-717.
- [16]. Guiying Song, Hexu Sun, Yi Zheng, “Study of the control strategy for mechatronics system of electric actuator”, *Intl. Conf on Electrical Machines and Systems*, Oct 07, pp 1584-1587.
- [17]. Economou, J.T. Luk, P.C.K., White, B.A. “Intelligent control of a multi-actuator mobile robot with competing factors”, *IEEE Conf. on Fuzzy Systems 2003*, May 2003, pp 302-306.
- [18]. Hungsun Son; Kok-Meng Lee, “Distributed Multipole Models for Design and Control of PM Actuators and Sensors”, *IEEE Transactions on Mechatronics*, Vol 13 No 2, April 2008, pp228-238.
- [19]. Aghili, F. Hollerbach, J.M. Buehler, M, “A Modular and High-Precision Motion Control System With an Integrated Motor”, *IEEE Trans. on Mechatronics*, June 2007, pp 317-329.
- [20]. Finite Element Method Magnetics: Home Page: Available at <http://femm.foster-miller.net>

- [21]. Eric Denisson: Available at <http://www.netdenizen.com/emagnet/offaxis/lopooffaxis.html>
- [22]. G. N. S. Prasanna, Gowthaman, and Manjunath Prasad, *Electrical Mechanisms : A merger of mechanisms and Electrical Machines*, in Proceedings of National Conference on Mechanisms and Machines, Bangalore, 2007.
- [23]. Haus, H and Melcher, *Electromagnetic Fields, Forces and Motion*, Prentice-Hall, Englewood Cliffs, NJ: Prentice-Hall, 1989. ISBN: 9780132490207.
- [24]. Jordan and Balmain, *Electromagnetic Waves and Radiating Systems*, Prentice-Hall, Englewood Cliffs, NJ,
- [25]. Boyd, *Convex Optimization*, Cambridge Univ Press, 2007.

#### APPENDIX A: RELATED WORK

Related work in motion control [10]-[12] generally separates the problem of designing a prime mover, from that of controlling the mechanism driven by it. The prime movers are generally either rotor or linear motors, and generally but not always there is only a single actuator in the mechanism. We generalize this to actuation at all joints and links in the mechanism leading to a merger of the identities of the mechanism and the prime movers. Such devices (emecs) can have better dynamics, fewer or no singularities, etc compared to mechanisms driven by classical prime mover - e.g. motors..

Specifically, in (Strete et al 1996 - [10]), a hybrid CAM mechanism with a constant velocity motor and a servo driving a CAM creating customizable dynamics is proposed. The paper says:

...Classical machines use a single motor, which generates all motions through a series of mechanical transmissions. Several mechanical components (such as linkages, cams, ...) transform the constant angular velocity of the motor in cyclic nonuniform motions, and assure also the synchronization between the different motions. ... The main disadvantage of the solution is its lack of flexibility ...

... Recently, the connection of a servo motor to a mechanism has been studied in order to combine the advantages of both the classical and the servo solutions. ... Hybrid machine ... (is a) servo motor and a constant velocity (CV) motor that are coupled through a two degree-of-freedom (DOF) mechanism and drive a single output. ...

Here the prime mover is still a servo motor/CV motor - an activated revolute pair in our framework, and requires active control to achieve customizable dynamics as exemplified by changing CAM timing. Our work, instead, changes the dynamics of the prime-mover-mechanism system, by treating the two as an *indistinguishable* unit, which can be designed as per Integral equation formulations, and cost effectively mass produced. The example of the IC engine flywheel shows the industrial applicability of the same.

The decoupling of the prime mover from the mechanisms is seen also in [11] and [12]- our framework couples the two. In [13] our methods can enable the disk

drive servo system to achieve controlled acceleration/forces (say max acceleration limited to 1000 m/s<sup>2</sup>) by the design of the mechanism enhanced with magnetics itself, and not necessarily due to active control. Hirose et al [7] describe how multiple actuators can be used to maximize power output or minimize energy of a robotic mechanism, but the actuators are still rotary or linear motors, and separate from the mechanism. Dixon [14] describes methods to control amplitude limited robot manipulators under uncertainty, but the actuators are all revolute. In [15], Boldea et al describe linear actuators - a powered prismatic pair in our framework. The torque ripple of the switched reluctance motor in [16] can be passively reduced using our methods, instead of by current control, potentially increasing efficiency. Our methods offer improvements to the control of the multi-actuator driven robot in [17] by changing the nature of the actuators themselves to reduce and/or eliminate the competition between the different actuators - the entire mechanism is designed as a coupled system. The multipole methods in [18] can be used to design the permanent magnets used, our work uses an approximate integral equation which is easy to solve. Our methods can be applied to design high precision positioning mechanisms, as opposed to a motor integrated with the mechanism in [19].